WEDNESDAY SLIDE CONFERENCE 2011-2012

Conference 23

02 May 2012

CASE I: S788/08 (JPC 3102484).

Signalment: 1.2-year-old female common squirrel monkey, *Saimiri sciureus*, New World monkey.

History: The animal showed severe dyspnea, apathy, hypothermia and mucous nasal discharge. In the oral cavity a mucous exudate and multifocal moderate gingival erosions were observed. The animal's condition worsened gradually and it died spontaneously.

Gross Pathology: At necropsy the body was in a moderate nutritional condition. In the oral cavity multifocal gingival ulcerations of 1 to 2 mm in diameter were observed. The lung showed severe congestion, moderate alveolar edema and multifocal hemorrhages of 2 to 4 mm in diameter. The spleen was moderately enlarged. The liver displayed moderate diffuse lipidosis. On the left shoulder (at the level of the supraspinatus muscle) a subcutaneous hemorrhage, 2 x 2 cm, was observed.

Laboratory Results:
Radiological findings: mild multifocal radiodense areas in the thoracic cavity.
Using an antibody against human Herpes simplex virus type 1, a strong positive reaction (Herpes simplex virus infection) was observed in tissue sections of the oral mucosa and liver.
Ultrastructurally, in hepatocytes intranuclear herpesviral nucleocapsids were observed.

Contributor's Histopathologic Description: The liver had a regular architecture. There were irregularly distributed, sublobular foci of coagulation necroses. Hepatocytes adjacent to the necrotic areas displayed cytoplasmic vacuoles of variable size interpreted as fatty degeneration. Furthermore, in some perilesional hepatocytes large eosinophilic intranuclear inclusion bodies causing chromatin margination and clumping were observed. The liver also displayed a mild to moderate, acute congestion.

Contributor's Morphologic Diagnosis: Liver: multifocal moderate acute coagulation necrosis with eosinophilic intranuclear inclusion bodies, and multifocal moderate hepatic lipidosis.

Contributor's Comment: In the submitted liver tissue, the main lesion consists of multifocal coagulation necrosis, and eosinophilic intranuclear inclusion bodies in adjacent hepatocytes.

Upon histological examination of other tissues, a severe multifocal ulcerative to necrotizing gingivitis with hydropic degeneration of epithelial cells, multinucleated giant cells (syncytia), eosinophilic intranuclear inclusion bodies, and a moderate necrotizing vasculitis was observed. The cerebellum showed a moderate subacute multifocal necrotizing inflammation with eosinophilic intranuclear inclusion bodies in neurons. The small intestine displayed a subacute multifocal moderate necrotizing enteritis with multinucleated cells (syncytia) and intranuclear
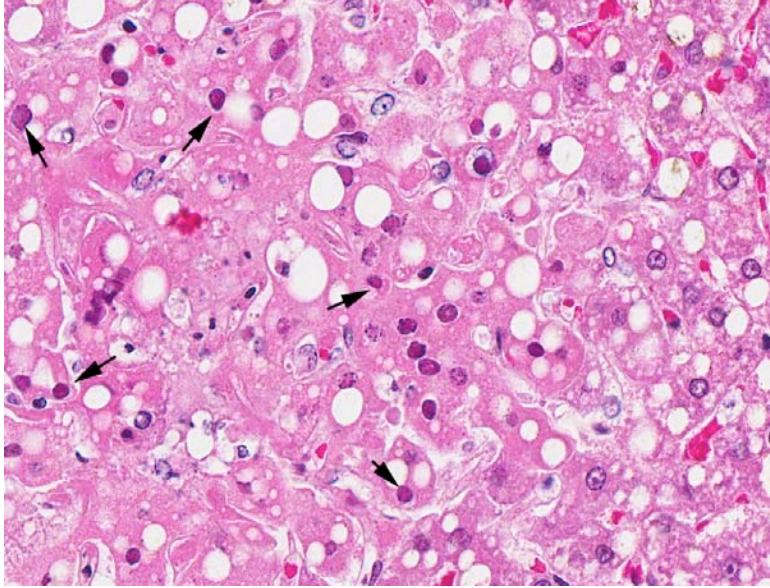
1-1. Liver, squirrel monkey: At the edges of the scattered foci of necrosis, degenerating hepatocytes contain a large magenta intranuclear viral inclusion that peripheralizes the chromatin. (HE 400X)

eosinophilic inclusion bodies in enterocytes. In the spiral ganglion of the ear, numerous eosinophilic intranuclear inclusion bodies were observed. The lymphoid tissues showed a severe lymphocytic depletion. In the nasal cavity a mild subacute diffuse purulent inflammation was present. In the lung, a mild multifocal subacute histiocytic pneumonia, moderate fibrin-rich alveolar edema, severe multifocal hemorrhages and severe congestion were found.

The detection of syncytia and eosinophilic intranuclear inclusion bodies as well as the ultrastructural demonstration of herpesviral nucleocapsids indicates a systemic herpesviral infection. Using immunohistochemistry an infection with human Herpes virus type 1 (HHV-1; Herpes simplex virus 1) was confirmed. Based on the ulcerative to necrotizing lesions, syncytia formation and the detection of eosinophilic intranuclear inclusion bodies in the mouth of the affected animal, an oral route of infection should be considered.

Herpesviruses are a family of large DNA viruses which infect humans, mammals, vertebrates and invertebrates.[1,9] The virions are 200-250 nm in diameter, consist of a linear double-stranded DNA genome of 120-240 kbp packaged in an icosahedral capsid approximately 125 nm in diameter, embedded in a matrix containing many viral proteins, itself wrapped in a lipid membrane containing several glycoproteins.[2,9] The family Herpesviridae is divided in three subfamilies Alpha-, Beta- and Gammaherpesvirinae on the basis of their genomic attributes.[2,9]

Nonhuman primates are primary hosts of a number of alpha- and gammaherpesviruses, whereas some host specific herpesviruses (e.g. Herpesvirus ateles, Herpesvirus saimiri, Rhesus rhadinovirus) were described.[2,8,11] In their natural hosts these viruses cause mild or inapparent infections, but they generally are associated with severe infections when interspecies transmission occurs.[3,4,10] The ability of herpesviruses to cross interspecies barriers is responsible for a major zoonotic risk of these pathogens.[5,8] Hence, the human herpesviruses are transmissible from humans to primates; however, spontaneous infections in monkeys appear to be rare.[5,8] In Old World primates, HHV-1 infections remain localized at the mucocutaneous tissues and the virus-host relationship is comparable to that of humans.[6,8] In contrast, New World monkeys and prosimians are more susceptible to infection and systemic disease.[5] In spontaneously infected owl monkeys, (*Aotus trivirgatus*), tree shrews (*Tupaia glis*), common marmosets (*Callithrix jacchus*), black-tufted-ear marmosets (*Callithrix penicillata*) and lemurs, a severe disease leading to death occurs in most cases.[8] In most mentioned species, erosions and ulcers of the oral mucous membranes and mucocutaneous junction of the lips, and focal necrosis and hemorrhage and eosinophilic intranuclear inclusion bodies were observed.[5,8] The source of the herpesvirus infection in nonhuman primates seems to be, in most cases, the close contact with persons shedding virions.[8] Close contact is also necessary for the transmission of the infection, hence most cases of herpesvirus infections in nonhuman primates occur in animals kept by private persons.[8] Therefore, the use of appropriate protective measures for humans handling nonhuman primates should greatly reduce the risk of infection.

JPC Diagnosis: 1. Liver: Hepatitis, necrotizing, multifocal and random, mild, with hepatocellular intranuclear viral inclusion bodies.
2. Liver, hepatocytes: Lipidosis, micro- and macrovesicular, diffuse, moderate.

Conference Comment: Herpes simplex (*Herpesvirus hominis*) has two distinct subtypes. Herpes simplex type 1 (HSV-1) causes oral lesions and encephalitis in adult humans, and HSV-2 causes genital lesions in adult humans and systemic disease in human infants. Both types produce the same fatal disease in New World monkeys.

Discussion during the conference was focused on developing a plausible differential diagnosis for these lesions in both New and Old World monkeys: Macaqacine herpesvirus (herpesvirus B), which causes fatal encephalomyelitis in man, produces similar lesions as seen in this case of necrotizing hepatitis as well as hemorrhagic necrosis in the lung, brain, and lymphoid organs. *Herpesvirus tamarinus* (herpesvirus T), which is asymptomatically carried by squirrel monkeys, and herpes simplex both cause identical necrotizing lesions in other New World monkeys such as aotus monkeys, marmosets, and tamarins. Virus isolation or immunohistochemical staining is necessary to differentiate them. Simian varicella virus causes similar necrotizing lesions with herpetic viral inclusions and syncitial cells of vesicular rash and encephalitis, pneumonia, and hepatitis in African green monkeys and other Old World monkeys.[7]

Contributor: University of Veterinary Medicine, Hannover
Department of Pathology
Bünteweg 17
D-30559, Hannover
Germany
http://www.tiho-hannover.de/
http://www.tiho-hannover.de/einricht/patho/index.htm

References:
1. Batista FM, Arzul I, Pepin JF, et al. Detection of ostreid herpesvirus 1 DNA by PCR in bivalve molluscs: a critical review. *J. Virol. Methods*. 2007;139 (1):1-11.
2. Davison AJ, Trus BL, Cheng N, et al. A novel class of herpesvirus with bivalve hosts. *J Gen Virol*. 2005;86,41-53.
3. Fickenscher H, Fleckenstein B. Herpesvirus saimiri. *Philos. Trans. R . Soc. Lond. B Biol. Sci*. 2001;356 (1408):545-567.
4. Hall KT, Giles MS, Goodwin DJ, et al. Characterization of the herpesvirus saimiri ORF73 gene product. *J. Gen. Virol*. 2000;81(Pt 11):2653-2658.
5. Juan-Sallés C, Ramos-Vara JA, Prats N, et al. Spontaneous herpes simplex virus infection in common marmosets (Callithrix jacchus). *J. Vet. Diagn. Invest*. 1997;9(3):341-345.
6. Kik MJ, Bos JH, Groen J, et al. Herpes simplex infection in a juvenile orangutan (Pongo pygmaeus pygmaeus). *J. Zoo. Wildl. Med*. 2005;36(1):131-4.
7. Mansfield K, King N. Viral diseases. In: Bennett BT, Abee CR, Henrickson R, eds. *Nonhuman Primates in Biomedical Research, Diseases*. San Diego, CA: Academic Press; 1998:5-12.
8. Mätz-Rensing K, Jentsch KD, Rensing S, et al. Fatal Herpes simplex infection in a group of common marmosets (Callithrix jacchus). *Vet Pathol*. 2003;40(4): 405-411.
9. McGeoch DJ, Dolan A, Ralph AC. Toward a comprehensive phylogeny for mammalian and avian herpesviruses. *J. Virol*. 2000;74(22):10401-1046.
10. Rootman DS, Haruta Y, Hill JM. Reactivation of HSV-1 in primates by transcorneal iontophoresis of adrenergic agents. *Invest Ophthalmol. Vis. Sci*. 1990;31 (3):597-600.
11. Schäfer A, Lengenfelder D, Grillhösl C, et al. The latency-associated nuclear antigen homolog of herpesvirus saimiri inhibits lytic virus replication. *J. Virol*. 2003;77(10):5911-5925.

CASE II: G7740 (JPC 3105937).

Signalment: 2-month-old intact female red-handed tamarin (*Saguinus midas*), nonhuman primate.

History: The animal belonged to a group of tamarins (*Saguinus midas*) on exhibit at a German Zoo. The group was established with one breeding couple. Reproduction has been successful and the female has given birth to 20 children. Out of these, two were born dead and six infants died within the first three month after birth. The group lived in an indoor-outdoor enclosure. The tamarin was one of two offspring of the year 2007. The other offspring was found dead 12 days earlier with similar symptoms. The parents remained clinically healthy. This monkey was euthanized due to a poor prognosis.

Gross Pathology: The tamarin was in a poor body condition. There was little content in stomach and intestinal tract. The great parenchymas were free of macroscopically conspicuous alterations. The brain was hyperemic with scattered foci of malacia.

Contributor's Histopathologic Description: Histopathologic examination revealed granulomas in brain, heart and liver. The granulomas occurred in all parts of the brain and were frequently found adjacent to small blood vessels. They consisted of macrophages, lymphocytes and few granulocytes. Protozoan organisms were found within the granulomas. They occurred free or within pseudocysts. Individual ovoid organisms measured 2.5 x 1.5 µm, pseudocysts were about 60 – 120 mm in diameter and contained numerous individual organisms. The lesions were followed by non-suppurative meningitis. Organisms were demonstrable within the meninges. The morphology of these organisms was consistent with microsporidia. Organisms of this type were also detected in other histologically unchanged organs. Pseudocysts and spores were gram positive and Giemsa positive single organisms in the pseudocysts reacted acid fast.

Immunohistochemistry: *Encephalitozoon cuniculi:* positive, provided by Prof. Pospischil, University Zürich, Switzerland

Immunohistochemistry for *Toxoplasma gondii:* negative

Contributor's Morphologic Diagnosis: CNS: encephalitis, granulomatous, subacute, multifocal, severe, with myriad intralesional and free laying protozoa, etiology consistent with *Encephalitozoon*
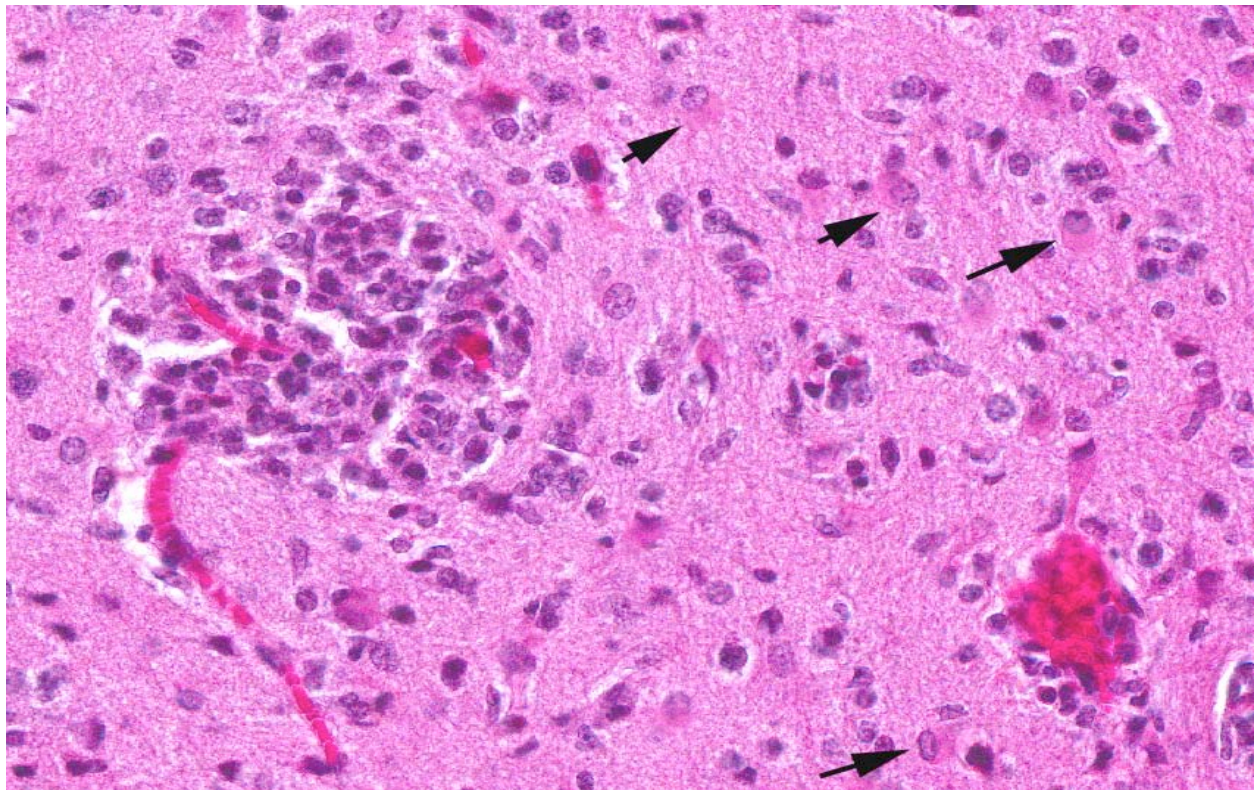

2-1. Cerebrum, tamarin: The gray matter contains numerous foci of necrosis which are filled with moderate numbers of histiocytes, often in perivascular areas. The adjacent neuropil exhibits gliosis, including numerous gemistocytic astrocytes (arrows). (HE 400X)

cuniculi, tamarin (*Saguinus midas*), nonhuman primate.

Contributor's Comment: Encephalitozoonosis is caused by *Encephalitozoon cuniculi*, an obligate intracellular protozoan parasite of the family *Pleistophoridae* and the phylum *Microspora*. *E. cuniculi* is a small oval parasite that measures 2.5 x 1.5 µm. The organism is characterized by a coiled polar filament in the mature spore stage. Ruptured mature spores release the organisms into the surrounding environment and infect other cells. The parasite is able to infect a variety of cell types but there is a predilection for macrophages, cells of the central nervous system and renal tubular epithelium. Spores are passed out with the urine.

Infections may be acquired horizontally or vertically. Infection of mammals most often occurs by ingestion or inhalation of contaminated urine or feces shed by the infected host. Transplacental transmission has also been described.

Microsporidia of the genus *Encephalitozoon* are well recognized pathogens in a wide range of hosts. *E. cuniculi* and other members of the microsporidial
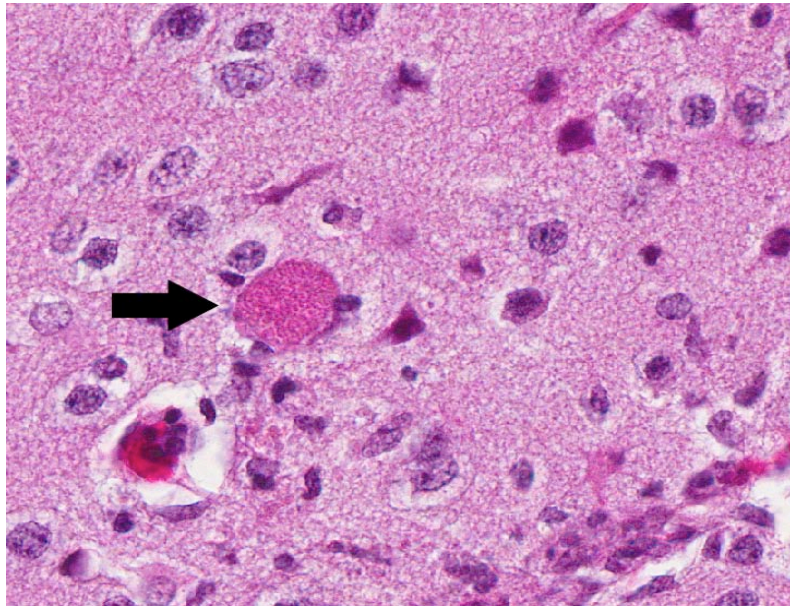
2-2. Cerebrum, tamarin: Throughout the neuropil are large, poorly-staining 60-140 µm pseudocysts containing numerous microsporidians, consistent with Encephalitozoon cuniculi. (HE 400X)

parasites have been regaining interest as opportunistic pathogens for individuals with a compromised immune system.

E. cuniculi is known for its widespread occurrence in rabbits and is an important opportunistic pathogen in HIV-infected immunocompromised humans. To date, three different *Encephalitozoon* species are identified. The different strains have different host preferences and were designated according to their main host as 'rabbit strain', 'mouse strain' and 'dog strain'. Furthermore, the three strains differ in their geographic distribution. The rabbit strain has a worldwide distribution, the mouse strain occurs in Europe only, and the dog strain has been identified in America and South Africa only.

Natural *E. cuniculi* infection may occur in nonhuman primates. Most reported cases involved different New World monkey species, mainly infant squirrel monkeys.[1,2,8] Furthermore, *E. cuniculi* was detected in emperor tamarins[3] and cotton top tamarins.[5] Clinically, signs of infected monkeys are usually absent or the animal develops nonspecific clinical disorders prior to death. The occurrence of latent infections is possible. Infections may be associated with stillbirths, abortions and perinatal deaths. *Encephalitozoon* infection in a colony can be diagnosed clinically by serologic investigation.[6]

Diagnosis can be made by finding the parasites and the typical associated lesions during histopathologic examination of the tissue or by demonstrating the agent in the urine. *E. cuniculi* must be differentiated from *Toxoplasma gondii* in histological sections. Staining properties of the organism and the nature of the inflammatory response can help to differentiate it from other infections. *E. cuniculi* stains poorly with hematoxylin and eosin, but stains well with Giemsa, Gram, periodic acid-Schiff (PAS) and Ziehl-Nielson. *Encephalitozoon* is gram-positive and variably acid fast, which is consistent with microsporidia and distinct from protozoa such as *Toxoplasma* or *Neospora*. *Toxoplasma* does not stain with a gram-stain. Furthermore, *Toxoplasma* cysts are smaller than *Encephalitozoon* pseudocysts, and individual *Toxoplasma* organisms are larger and crescent shaped, while *Encephalitozoon* is smaller and ovoid.[2]

Electron microscopy can reveal the presence of the typical parasitophorous vacuoles as well as the distinctive polar filaments. The polar filament may be coiled up to six times around the inner wall of the spore or may be extruded. Immunological or molecular techniques are best suited to distinguish between different protozoan species and strains.

JPC Diagnosis: Brain: Meningoencephalitis, granulomatous, multifocal, marked, with gliosis and numerous microsporidian pseudocysts.

Conference Comment: *Encephalitozoon* exhibits selective parasitism of vascular endothelium, especially in the brain and kidney, as well as renal tubular epithelium. Spores, which are the infective stage, usually obtain entry through the digestive tract, and the sporoplasm, which contains the genetic material, is either released and engulfed by macrophages or injected into endothelial cells through the extruded polar filament. Asexual replication occurs to form numerous proliferative meronts, which differentiate into sporoblasts and then sporonts. A dense spore wall is produced over the plasma membrane, which thickens and allows spore organelles to form. Spores are then packaged within a parasitophorous vacuole, which enlarges and causes host cell rupture. There is release of spores into the extracellular spaces, which then can infect adjacent cells, or enter the vascular system or the renal tubular lumen to be passed in the urine.[4,7]

Typical gross lesions in nonhuman primates include granulomatous meningoencephalitis and vasculitis, nonsuppurative interstitial nephritis and pneumonia, and granulomatous placentitis. A "classic" gross lesion in the rabbit is multifocal irregularly depressed pits in the kidneys with indistinct linear pale gray-white streaks on cut surface. In severe cases, hydrocephalus, thrombosis of meningeal blood vessels, and focal encephalomalacia can occur.[2,4,7] In the dwarf rabbit, which is especially susceptible, *E. cuniculi* has been associated with phacoclastic uveitis and cataract formation, in addition to meningoencephalomyelitis and radiculoneuritis.[4]

In addition to the electron microscopy findings of a parasitophorous vacuole and coiled polar filament mentioned by the contributor, a corrugated proteinaceous electron dense exospore, a chitinous radiolucent endospore, an anchoring disc at the anterior pole, and an electron lucent posterior vacuole are present.[7]

Contributor: German Primate Center
Department of Infectious Pathology
Kellnerweg 4
37077 Göttingen
Germany
http://dpz.eu

References:
1. Asakura T, Nakamura S, Ohta M, et al. Genetically unique microsporidian *Encephalitozoon cuniculi* strain type III isolated from squirrel monkeys. *Parasitol. Intern*. 2006;55:159 -162.
2. Baskin G. *Enzephalitozoon cuniculi* infection, squirrel monkey. In: TC Jones TC, Mohr U, Hunt RD, eds. *Nonhuman Primates II*. 1993;193-196.
3. Guscetti F, Mathis A, Hatt J-M, et al. Overt fatal and chronic subclinical *Encephalitozoon cuniculi* microsporidiosis in a colony of captive emperor tamarins (*Saguinus imperator*). *J. Med. Primatol*. 2003;32:111-119.
4. Percy DH, Barthold SW. Pathology of Laboratory Rodents and Rabbits. 3rd ed. Ames, IA: Blackwell Publishing; 2007;290-4.
5. Reetz J, Wiedemann M, Aue A, et al. Disseminated lethal *Encephalitozon cuniculi* (genotype III) infections in cotton-top tamarins (*Oedipomidas oedipus*) – a case report. *Parasitol. Intern*. 2004;53:29–34.
6. Shadduck JA, Baskin G. Serologic evidence of *Encephalitozoon cuniculi* infection in a colony of squirrel monkeys. *Lab. Anim. Sci*. 1989;39:328–330.
7. Wasson K, Peper RL. Mammalian microsporidiosis. *Vet Pathol*. 2000;37(2):113-28.
8. Zeman DH, Baskin G. Encephalitozoonosis in squirrel monkeys (*Saimiri sciureus*). *Vet Pathol*. 1985;22:24–31.

CASE III: 10A089 (JPC 4002933).

Signalment: 8.74-year-old female Indian Rhesus macaque (*Macaca mulatta),* nonhuman primate.

History: This animal was part of a routine SHIV study, at the end of which it was euthanized for tissue collection. Clinically normal animal, incidental finding at necropsy.

Gross Pathology: A 5.5 X 4.5 X 3 cm, irregularly round, whitish, sessile, expansile, soft mass, with bosselated but smooth external surface and no adhesions to the adjacent structures, is identified on the right ovary. The cut surface is light tan-to-beige, smooth and relatively soft, with a few irregularly-shaped, non-intercommunicating cyst-like structures. The left ovary along with the rest of genital tract is grossly normal. All other organs are within normal limits.

Contributor's Histopathologic Description: Right ovary: About 98% of the ovarian parenchyma is completely effaced and replaced by an unencapsulated, infiltrative, and densely to sparsely cellular neoplasm, compressing preexisting ovarian stroma and pre-antral and antral follicles present in the periphery between the neoplasm and ovarian tunica albuginea , and sparing the oviduct (not present in all slides). Neoplastic cells are arranged in sheets,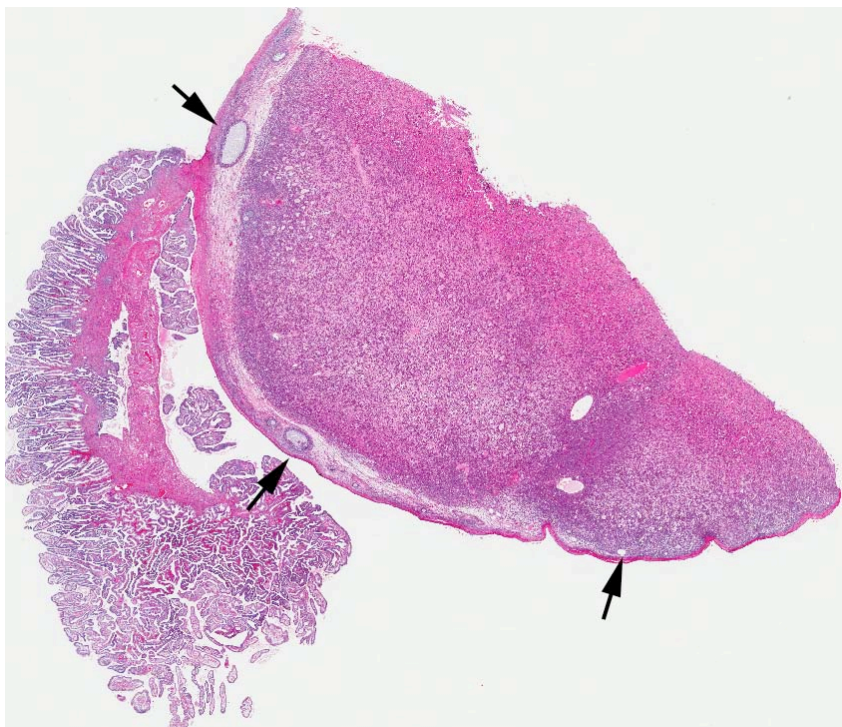 islands, nests, strands, and cords of round-to-polygonal cells (germ cells) separated by fine fibrovascular stroma, which is expanded in many areas by varied amount of slightly eosinophilic lacy-to-amorphous material (secretory protein/edema). Neoplastic cells have distinct to indistinct cell borders, minimal-to-abundant eosinophilic granular cytoplasm, large round, centrally located, and vesicular nuclei with finely stippled chromatin and a single magenta nucleolus. Multifocally, neoplastic cells surround numerous variably-sized cyst-like spaces that are usually filled with proteinaceous fluid and occasionally contain small amount of lacy material admixed with a few neoplastic cells, lymphocytes, neutrophils and cellular debris and tend to form binucleated-to-multinucleated cells with up to 5 nuclei. Mitotic figures are common (average 3-4 per HPF), some of which are atypical, and there is marked anisocytosis and anisokaryosis. Interspersed among neoplastic cells are multifocal accumulations of lymphocytic infiltrate, clusters of interstitial gland cells with large vacuolated cytoplasm, variably distinct borders, and central-to-eccentric nucleus, scattered single cell necrosis, low numbers of plasma cells and neutrophils, and occasional eosinophils. Variably-sized masses of neoplastic cells are present within lymphatic vessels, and there are focal areas at the periphery of the mass where neoplastic cells tend to breach the adjacent tunica albuginea. Edema and some mineralized foci are also noted.

3-1. Ovary and fimbria, rhesus monkey: The majority of the ovary is replaced by an infiltrative neoplasm (dysgerminoma). Several remaining follicles are present at the edge of the ovary (arrows). (HE 4X)
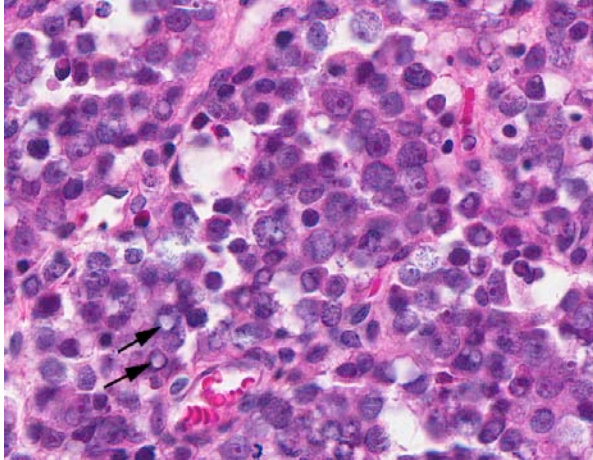
Immunohistochemistry:
- Vimentin, multifocally weakly positive.
- Cytokeratin, negative.
- Alpha-fetoprotein, negative.
- CD3, negative for neoplastic cells; positive for lymphocytic infiltrate.

**Contributor's Morphologic Diagnosis:** Right ovary: dysgerminoma, rhesus monkey *(Macaca mulatta).*

Contributor's Comment: An incidental finding of unilateral ovarian dysgerminoma in a rhesus monkey *(macaca mulatta)* is examined histologically and immunohistochemically. To our knowledge there is only one documented report of ovarian dysgerminoma in a rhesus monkey.[6] Ovarian dysgerminomas and seminomas, their testicular analogue, are germ cell tumors that arise from primordial germ cells of the ovary

3-2. Ovary, rhesus monkey: The neoplasm is composed of germ cells with large nuclei, prominent nuclei, and often, clear cytoplasmic invaginations into the nucleus (arrows). (HE 400X)
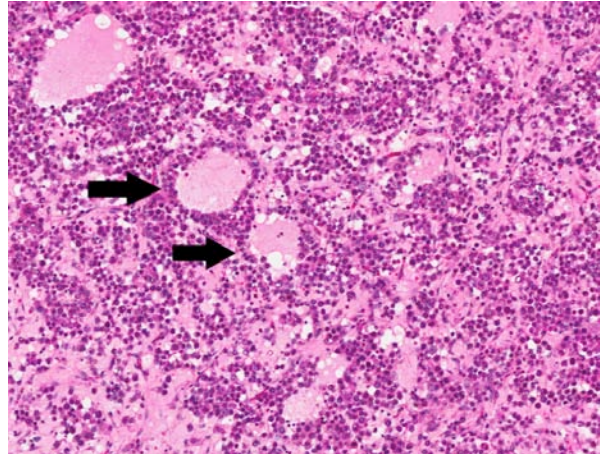
3-3. Ovary, rhesus monkey: Centrally, there is marked edema, apoptosis, and necrosis with dropout (arrows) separate neoplastic cells and cause a bit of diagnostic confusion if only this portion of the slide was viewed. (HE 100X)

and the testis. In female domestic animals, germ cell tumors are limited to germinoma and teratomas, whereas in women and female laboratory animals other ovarian germ cell neoplasms also include: embryonal carcinoma, choriocarcinoma, and endodermal sinus tumor.[7] Although rare, ovarian dysgerminomas are reported in a variety of mammals and non-mammalian species, including humans (girls and women)[9]; non-human primates[6]; domestic animals[7]; and wildlife, avian, amphibian and reptilian species and fishes.[11] Macroscopically, microscopically and immunohistochemically changes observed in this case are basically similar to those previously reported in other mammals and lower vertebrates.[11,4] Grossly, the neoplasm is usually unilateral but may be bilateral, relatively soft, with smooth external surface, and may have cystic structures on cut surface. Histologically, the neoplasm is usually diffusely densely cellular with focal cystic and mineralized areas and high mitotic index, and neoplastic cells are round to polygonal with granular cytoplasm. Interestingly in this case, the neoplasm is relatively less densely cellular but contains abundant amount of extracellular proteinaceous material consistent with accumulation of protein secretion and/or edema. Although not prominent in this case, some neoplastic germ cells express vimentin in perinuclear pattern, but no expression of cytokeratin, alpha-fetoprotein, or CD3 can be detected by immunohistochemistry. On histopathological examination, differential diagnosis should include any round cell neoplasm, especially lymphosarcoma. In general, ovarian dysgerminomas are considered to be nonfunctional in all species; however, they can be hormonally active.[2]

More recently, stem cell markers such as OCT3/4, SOX2, and growth differentiation factor 3 (GDF3) have been reported to be expressed variably in germ cell tumors.[4] Unfortunately, these markers expression could not be investigated in this case. The exact cause of dysgerminomas has not been determined, but more recent molecular studies[3] have implicated loss of function with potential tumor suppressor gene *TRC8/RNF-139* as a possible cause in humans. This would shed some light on the molecular pathways involved in the pathogenesis of this neoplastic condition, which remains to be determined.

JPC Diagnosis: Ovary and oviduct: Dysgerminoma.

Conference Comment: Dysgerminomas are considered potentially malignant, although they metastasize in only 10-20% of cases. Ovarian dysgerminomas are considered to arise from the follicular oocytes or testicular homologues within the ovary, in addition to primordial germ cells. The neoplastic cells share ultrastructural similarity to normal fetal oogonia. These neoplasms typically exhibit cytoplasmic and membranous immunoreactivity for placental alkaline phosphatase (PLAP), which is also positive in other malignant germ cell tumors, and is mainly useful in differentiating it from non-germ cell tumors such as clear cell carcinoma, malignant lymphoma, and granulosa cell tumor. Dysgerminomas also show membrane staining for CD117 (c-kit), which helps to differentiate them from embryonal carcinomas and yolk sac neoplasms. The stem cell-related protein Oct-4 mentioned by the contributor is also positive in embryonal carcinomas, although it is highly sensitive for dysgerminoma. However, podoplanin, which exhibits strong cytoplasmic immunoreactivity for dysgerminoma, can be used to rule out embryonal carcinoma, in which it is negative. The oncofetal glycoprotein alpha-fetoprotein mentioned by the contributor as negative for dysgerminoma is a positive marker for yolk sac

tumors. Many of these immunohistochemical markers are not widely available for veterinary diagnostics; therefore, CD117 may be the most useful and available marker to definitively prove dysgerminoma.[10]

Dysgerminomas have been reported in related maned wolves (*Crysocyon brachyurus*), which may have a genetic predisposition to these neoplasms, as well as in mountain chicken frogs (*Leptodactylus fallax*). In horses, dysgerminoma has been reported as a cause of hypertrophic osteopathy, which is more commonly associated with concurrent thoracic disease.[1,5,8]

Contributor: Tulane National Primate Research Center
Division of Comparative Pathology
18703 Three Rivers Road
Covington, LA 70433-8915

References:
1. Chandra AM, Woodard JC, Merritt AM. Dysgerminoma in an Arabian filly. *Vet Pathol*. 1998;35(4):308-11.
2. Gelberg HB, McEntee K. Feline Ovarian Neoplasm. *Vet Pathol*. 1985;22:577-576.
3. Gimelli S, Beri S, Drabkin HA, et al. The tumor suppressor gene *TRC8/RNF139* is disrupted by a constitutional balanced translocation (8;22)(q24.13;q11.21) in a young girl with dysgerminoma. *Molecular Cancer*. 2009;8:52.
4. Goplan A, Dhall D, Olgac S, et al. Testicular mixed germ cell tumors: a morphological and immunohistochemical study using stem cell markers, OCT3/4, SOX2 and GDF3, with emphasis on morphologically difficult-to-classify areas. *Modern Pathology*. 2009;22:1066-1074.
5. Fitzgerald SD, Duncan AE, Tabaka C. Ovarian dysgerminomas in two mountain chicken frogs (*Leptodactylus fallax*). *J Zoo Wildlife Med*. 2007;38(1):150-153.
6. Holmberg CA, Sesline D, Osburn, B. Dysgerminoma in a Rhesus Monkey: Morhologic and Biological Features. *J. Med. Primatol*. 1978;7:53-58.
7. Maclachnan NJ, Kennedy PC. Tumors of the genital systems. In: Meuten D, ed. Tumors in Domestic Animals. 4th ed. Ames, IA; Blackwell Publishing: 2002;547-557.
8. Munson L, Montali RJ. High prevalence of ovarian tumors in maned wolves (*Chrysocyon brachyurus*) at the National Zoological Park. *J Zoo Wildlife Med*. 1991;22(1):125-129.
9. Pectasides D, Pectasides E, Kassanos D. Germ cell tumors of the ovary. *Cancer Treat. Rev*. 2008;34(5):427-41.
10. Rabban JT, Soslow RA, Zaloudek CZ. Immunohistology of the female genital tract. In: Dabbs DJ, ed. *Diagnostic Immunohistochemistry, Theranostic and Genomic Applications*. 3rd ed. Philadelphia, PA: Saunders-Elsevier; 2010:737-8.
11. Strunk A, Imai DM, Osofsky A, et al. Dysgerminoma in an eastern rosella *(Platycercus eximius exemius)*. *Avian Diseases*. 2011;55:133-138.

CASE IV: 070347-7 (JPC 4006378).

**Signalment:** Adult male African green monkey (*Chlorocebus aethiops*).

History: These monkeys were part of a study characterizing pathologic changes associated with aerosolized tularemia. Theses monkeys received an average inhaled dose of 729 colony-forming units of *Francisella tularensis (F. tularensis*) and died or were euthanatized between days 7 and 11 postinfection. Clinical changes were evident by 48 hours postinfection, and key physiologic abnormalities included increases in body temperature, heart rate, peak cardiac pressure, and mean blood pressure.[15]

Gross Pathology: Prominent gross changes in all cases included numerous pinpoint to 1-cm, well-demarcated, necrotic foci present consistently in the lungs, mediastinal lymph nodes, and spleen but also seen in the heart, mediastinum, diaphragm, liver, urinary bladder, urethra, and mesentery. The lungs, mediastinal lymph nodes, and spleen were most severely affected, with as much as 50% of the tissue replaced by necrotic foci.

Laboratory Results: Immunohistochemical labeling demonstrated strong *F. tularensis* immunoreactivity in the cytoplasm of multiple cell types but was especially prominent within macrophages of the tonsil; mandibular, mediastinal, mesenteric, axillary, and inguinal lymph nodes; and in alveolar macrophages. Strong *F. tularensis* immunoreactivity was also observed in the following cell types: pleural mesothelial cells; respiratory epithelial cells of the larynx, trachea, bronchi, and bronchioles; epicardial cells; degenerating hepatocytes; reticuloendothelial cells and macrophages in the spleen; glomerular mesangial cells and/or endothelial cells; a variety of cell types in the bone marrow; cortical cells of the adrenal gland; the epithelium of the urinary bladder and urethra; and neutrophils and macrophages infiltrating multiple tissues. In addition, granular or amorphous extracellular antigen was evident in areas of necrosis or pyogranulomatous inflammation in multiple tissues.[15]

Electron microscopy was performed on the lung of one African green monkey (AGM). Organisms were readily identified within membrane-bound vacuoles within the cytoplasm of alveolar macrophages adjacent to the nucleus. The bacteria varied in shape but were generally oval or elongate and measured 0.4 to 0.5 mm in width. Bacteria contained a thin cell wall, a pale central cytoplasm, and a darker rim of cytoplasm near the cell wall. An outer membrane was present in some organisms and appeared as an irregular or wavy membrane loosely surrounding the organism. Many cells containing internal bacilli were seen in various stages of degeneration characterized by swollen irregular mitochondria with faded or absent internal cristae, cytoplasmic vacuoles, enlarged membrane-bound vacuoles with indistinct borders (with or without bacteria), disrupted smooth and rough endoplasmic reticulum, disrupted Golgi apparatus, and disrupted cell membranes. Because severe degeneration and necrosis often hindered recognition of these small bacteria, we used immunoelectron microscopy to distinguish organisms. The identification of *F. tularensis* was made with confidence when the bacterial cell wall contained black
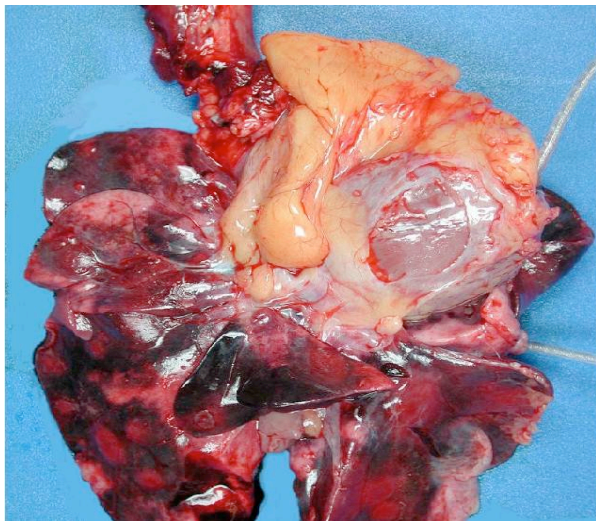

4-1. Lung, African green monkey: Up to fifty percent of the lung is replaced by foci of necrosis and suppuration. (Photo courtesy of the Division of Pathology, United States Army Medical Research Institute of Infectious Diseases (USAMRIID), Frederick, Maryland.)

4-2. Lung, African green monkey: The spleen contains numerous 0.1 to 0.2 cm diameter, raised, white lesions. Splenic borders are rounded, indicating marked congestion. (Photo courtesy of the Division of Pathology, United States Army Medical Research Institute of Infectious Diseases (USAMRIID), Frederick, Maryland.)
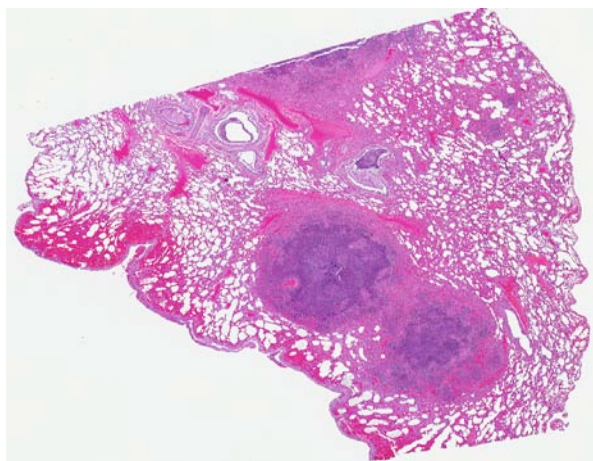
4-3. Lung, African green monkey: Large areas of necrosis efface airways and extend into surrounding tissue. (HE 40X)
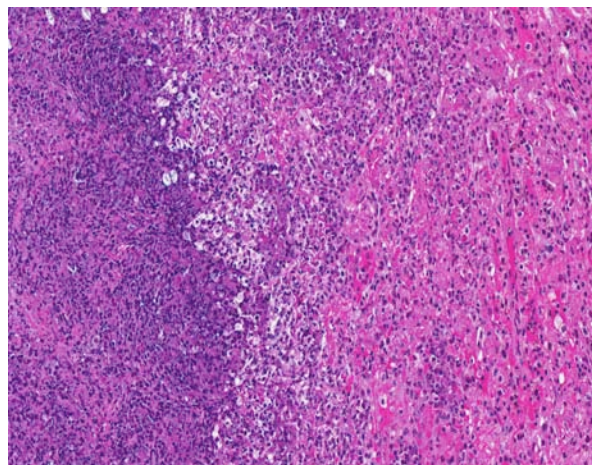
4-4. Lung, African green monkey: Foci of lytic necrosis (left) transition to consolidated pulmonary parenchyma (right). (HE 400X)

grains of gold particles that were evenly distributed over the entire bacterium.[15]

Contributor's Histopathologic Description: Histologic changes in all tissues consisted of well delineated foci of necrosis and neutrophilic and histiocytic inflammation, with varying amounts of hemorrhage, edema, fibrin, and vasculitis. Some lesions were immature pyogranulomas.

Contributor's Morphologic Diagnosis: Lung: Bronchopneumonia, necrotizing, multifocal, marked, with hemorrhage, edema, necrohemorrhagic pleuritis, multifocal necrotizing vasculitis, and rare thrombi.

Contributor's Comment: *Francisella tularensis* is a small pleomorphic gram-negative coccobacillus and is the causative agent of tularemia, also known as "rabbit-fever." Tularemia is a sporadic zoonotic disease in humans, and most cases in the USA are concentrated in south central and western states, primarily in rural areas of Arkansas, Missouri, and Oklahoma.[2] An enzootic life cycle of *F. tularensis* exists among wildlife, particularly involving rabbits, hares, and rodents. Humans may become infected through arthropod bites, through intact skin by handling infected animal carcasses, by ingesting contaminated food or water, or by inhaling contaminated aerosols.[7] *F. tularensis* is a highly virulent bacterium, with as few as 10 organisms constituting an infectious dose, and it can survive for long periods in the environment.[7,12] Most naturally acquired human cases can be successfully treated if it is diagnosed early and the patient is maintained on antibiotics for extended periods.[5]

Tularemia has been placed on the Centers for Disease Control and Prevention list of Class A biothreat agents. In natural cases, pneumonic tularemia is often a consequence of inhalation of bacteria. In a biowarfare or bioterrorism event involving *F. tularensis*, it is very likely that the bacteria would be disseminated via aerosolization, resulting in a high incidence of pneumonic tularemia.[7] Pneumonic tularemia presents some particular challenges relative to other forms (ulceroglandular, glandular, oculoglandular, oropharyngeal, typhoidal, and septic) of the disease. For instance, the antibiotic regimens most applicable for the treatment or postexposure prophylaxis of pneumonic tularemia, especially in a mass casualty event, are not completely certain. Also, vaccines that protect against ingestional or transdermal infection may not protect against high doses of inhaled bacteria.[10] Further, the correlates of immune protection against aerosolized *F. tularensis* have not been established with certainty. Therefore, appropriate animal models of aerosolized tularemia are required to develop the necessary medical countermeasures.[15]

The monkeys in this study exhibited a number of similarities to human tularemia, in particular with regard to the pneumonic form of disease. The key pathologic features of inhalational tularemia in these monkeys were numerous and widespread necrotizing pyogranulomatous lesions that especially targeted the lungs and lymphoid tissues. Bacteria were present in many cell types but were most readily present in alveolar macrophages, as well as macrophages in other tissues. Ultrastructural features included the presence of bacteria within cytoplasmic vacuoles that were located adjacent to the nucleus (*Francisella*-containing vacuoles),[4] as well as degenerative changes in infected cells. In addition, all five AGMs in our study had significant pleuritis associated with the lung lesions, representing another feature in common with the human counterpart, and one also shared by the rhesus macaque model.[7,8] Likewise, our finding that most lesions were characterized by necrosis combined with
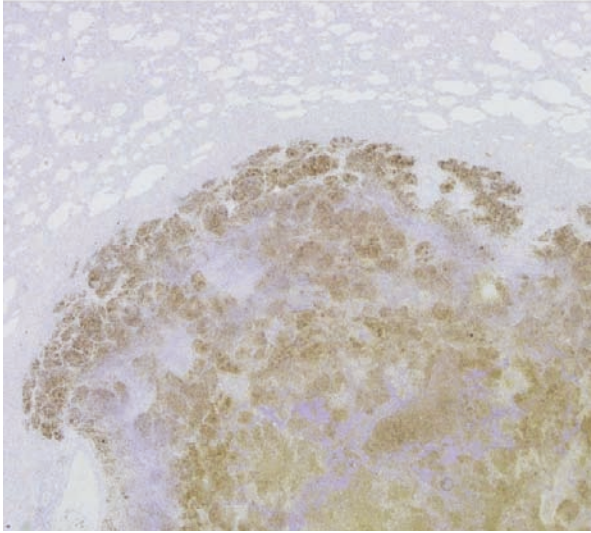
4-5. Lung, African green monkey: Alveolar macrophages and neutrophils exhibit marked immunoreactivity for F. tularensis.
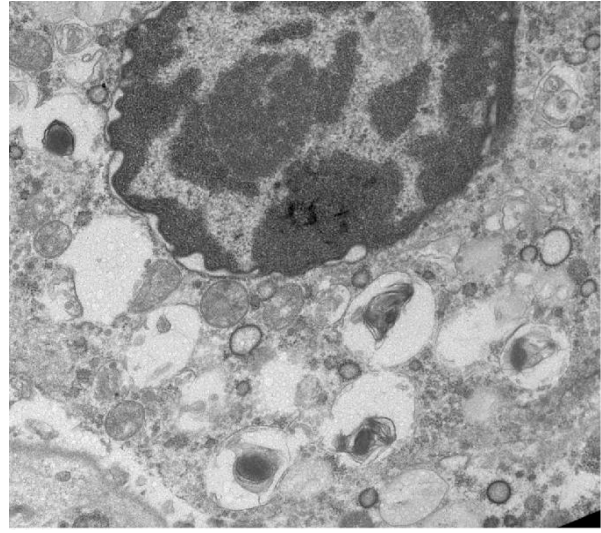
4-6. Lung, African green monkey: Electron micrograph of an alveolar macrophage with several intracytoplasmic vacuoles containing F. tularensis bacteria. The wavy, lamellated cell membranes are characteristic of this bacterium when phagocytosed.

neutrophilic and histiocytic inflammation progressing to form immature pyogranulomas is consistent with histologic findings in most forms of human tularemia, except the typhoidal form.[15]

Two differences between the disease in AGMs and that in humans were noted. We did not observe granulomas associated with epithelioid macrophages and multinucleated giant cells in the target organs of AGMs. It is possible that the monkeys in this study succumbed to disease before such lesions had sufficient time to fully develop. Another exception is that the kidney is a reported target of human tularemia, yet none of our cases displayed gross or histologic changes in the kidney. We did observe, however, that most kidneys had positive immunohistochemistry labeling (for bacterial antigen) within glomerular mesangial and/or endothelial cells. The importance of positive staining in the absence of pathologic changes in the tissue is unclear. One report did describe histologic changes in the renal glomeruli of rhesus macaques.[8] It is uncertain if the renal lesions provide a significant contribution to the pathogenesis in human tularemia in the face of the significant bacterial burden and lesions in the pulmonary and lymphoid systems, as well as other key organs.[15]

Our finding that *F. tularensis* was found in abundance in macrophages in the lungs, lymphoid tissues, and other tissues is a feature of the disease in AGMs with potentially critical significance to understanding the human condition. The ability of *F. tularensis* to infect macrophages, evade the immune system by preventing phagolysosome fusion, and then replicate in these cells is considered a key aspect of its pathogenesis.[3]

Infected macrophages also appear to be important in the pathogenesis of tularemia in that they secrete both proinflammatory and anti-inflammatory cytokines,[13] although a full understanding of the host and pathogen factors that operate within infected macrophages is lacking. Nonetheless, the AGM may provide a useful experimental model for investigating the nature of host-pathogen interactions in macrophages, as well as other aspects involved in the pathogenesis of tularemia.[15]

There are limited numbers of documented reports of experimental aerosolized tularemia in rhesus macaques, mostly dating back to the 1960s. These reports describe acute bronchiolitis progressing to bronchopneumonia, lymphadenitis, splenitis, and hepatitis with neutrophilic and histiocytic inflammation with intrahistiocytic bacteria.[6,8,14,17] Such features are similar to those seen in the AGMs of our study. Rhesus macaques have become increasingly expensive and limited in supply in recent years, which limits their usefulness as a model of tularemia. The most recent report of tularemia in nonhuman primates documents an epizootic of tularemia in a group of cynomolgus macaques (*Macaca fascicularis*) that contracted oropharyngeal tularemia by ingesting contaminated food and water. The tularemic lesions were present in the oral mucosa, tongue, lungs, liver, spleen, and lymph nodes consistent with ingestional human tularemia.[11] Therefore, the AGM model of inhalational tularemia we describe appears to share important features of the human condition and thus should provide a useful nonhuman primate model for future research. It is essential to continue to characterize the clinical and pathologic changes that occur in animal models of tularemia, as well as the

molecular mechanisms involved in this disease. Future experimental studies to develop early preventive regimens, early diagnostic procedures (identifying target organs for sampling), and clinical algorithms to optimize treatment efficacy will depend on reliable animal models that consistently mimic human disease. Likewise, relevant animal models will also be necessary to investigate avenues of altering pathogen and host factors, to include novel antibiotic therapies, immunomodulators, or inflammatory inhibitors. In that light, the AGMs reported here displayed consistent gross and histologic lesions after exposure to aerosolized *F. tularensis* with important parallels to human tularemia. This species of nonhuman primate may serve as a suitable and reliable animal model for further studies with *F. tularensis.*[15]

JPC Diagnosis: Lung: Bronchopneumonia, necrosuppurative, multifocal, severe, with fibrinous pleuritis.

Conference Comment: There are three strains that cause tularemia: *Francisella tularensis var tularensis*, the most virulent and commonly isolated form, *F. tularensis var holoarctica*, and *F. tularensis var mediasiatica*. Naturally acquired tularemia is rare in nonhuman primates, although a few recent outbreaks in New World monkeys have been reported in the United States and Europe. Typical gross findings include pyogranulomatous pneumonia and enteritis; necrosuppurative glossitis and gingivitis; and necrotizing splenitis, lymphadenitis, and hepatitis. Tularemia is difficult to differentiate from other causes of gram negative sepsis and often causes lesions indistinguishable from those of *Yersinia pseudotuberculosis*, a top differential diagnosis for this case; however, unlike *F. tularensis, Y. pseudotuberculosis* often forms large botryoid colonies of extracellular coccobacilli.[11,15,16]

Contributor: USAMRIID
Pathology Division
Attn: MCMR-UIP
1425 Porter Street
Fort Detrick, MD 21702

References:
1. Baskerville A, Hambleton P, Dowsett AB. The pathology of untreated and antibiotic-treated experimental tularaemia in monkeys. *Br J Exp Pathol.* 1978;59(6):615–623.
2. Boyce JM. Recent trends in the epidemiology of tularemia in the United States. *J Infect Dis.* 1975;131 (2):197–199.
3. Butchar JP, Rajaram MVS, Ganesan LP, et al. Francisella tularensis induces IL-23 production in human monocytes. *J Immunol.* 2007;178:4445–4454.
4. Checroun C, Wehrly TD, Fischer ER, et al. Autophagy-mediated reentry of *Francisella tularensis* into the endocytic compartment after cytoplasmic replication. *Proc Natl Acad Sci USA.* 2007;103(39): 14578–14583.
5. Cross JT, Penn RL. *Francisella tularensis* (tularemia). In: Mandell GL, Bennett JE, Dolin R, eds. Principles and Practice of Infectious Diseases. 5th ed. Philadelphia, PA: Churchhill Livingstone; 1999:2393–2401
6. Day WC, Berendt RF. Experimental tularemia in *Macaca mulatta*: relationship of aerosol particle size to the infectivity of airborne *Pasterurella tularensis. Infect Immun.* 1972;5(1):77–82.
7. Dennis DT, Inglesby TV, Henderson DA, et al. Tularemia as a biological weapon: medical and public health management. *JAMA.* 2001;285(21):2763–2773.
8. Hall WC, Kovatch RM, Schricker RL. Tularaemic pneumonia: pathogenesis of the aerosol-induced disease in monkeys. *J Pathol.* 1973;110:193–201.
9. Hartings JM, Roy CJ. The automated bioaerosol exposure system: preclinical platform development and a respiratory dosimetry application with nonhuman primates. *J Pharmacol Toxicol Methods.* 2004;49:39–55.
10. Hepburn MJ, Friedlander AM, Dembek ZF. Tularemia. In: Textbooks of Military Medicine, Aspects of Biological Warfare. Fort Sam Houston, TX: Borden Institute, Office of the Surgeon General, United States Army Medical Department Center and School; 2007:167-184.
11. Mätz-Rensing K, Floto A, Schrod A, et al. Epizootic of tularemia in an outdoor housed group of cynomolgus monkeys (Macaca fascicularis). *Vet Pathol.* 2007;44(3):327–334.
12. Nayar GP, Crawshaw GJ, Neufeld JL. Tularemia in a group of nonhuman primates. *J Am Vet Med Assoc.* 1979;175(9):962–963.
13. Rajaram MV, Ganesan LP, Parsa KV, et al. Akt/PKB modulates macrophage inflammatory response to *Francisella* infection and confers a survival advantage in mice. *J Immunol.* 2006;177:6317–6324.
14. Schricker RL, Eigelsbach HT, Mitten JQ, et al. Pathogenesis of tularemia in monkeys aerogenically exposed to *Francisella tularensis* 425. *Infect Immun.* 1972;5(5):734–744.
15. Twenhafel NA, Alves DA, Purcell BK. Pathology of inhalational *Francisella tularnesis* spp. Tularnesis SCHU S4 infection in African green monkeys (*Chlorocebus aethiops*). *Vet Pathol.* 2009;46:698-706.
16. Valli VEO. Hematopoietic system. In: Maxie MG, ed. *Jubb, Kennedy, and Palmer's Pathology of Domestic Animals.* 5th ed. vol 3. Philadelphia, PA: Elsevier; 2007:297-9.
17. White JD, Rooney JR, Prickett PA, et al. Pathogenesis of experimental respiratory tularemia in monkeys. *J Infect Dis.* 1964;114:277–283.